



# SAR IMAGE ENHANCEMENT FOR SMALL TARGET DETECTION

Jingxin Zhang<sup>†</sup> Jim Schroeder<sup>‡</sup> Nicholas J. Redding<sup>§</sup>

<sup>†</sup> School of Engineering and Technology, Deakin University, Geelong Vic 3217, Australia

Tel: +61-3-5227 1373, Fax: +61-3-5227 2140, Email: jingxz@deakin.edu.au

<sup>‡</sup> DSpace Pty Ltd, Innovation House West, Technology Park, Mawson Lakes, SA 5095, Australia

<sup>§</sup> Defence Science and Technology Organisation, P.O. Box 1500, Edinburgh, SA 5111, Australia

## ABSTRACT

This paper investigates the impact of SAR image enhancement on the performance of small target detection in SAR images. Three SAR image enhancement algorithms are evaluated on large SAR image data-sets. The evaluation results show that image enhancement can greatly improve the performance of false alarm mitigation, and that the level of performance improvement is correlated with the resolution and background suppression of the enhanced images. The higher the resolution and the level of background suppression, the higher the level of performance improvement.

## 1. INTRODUCTION

Enhancement of synthetic aperture radar (SAR) images reduces speckle, increases signal-to-noise ratio, enhances dominant domain features [1, 3, 2, 4, 5], and improves greatly the performance of automatic target recognition (ATR) in SAR images [7, 8, 9].

In [7, 8, 9], image enhancement is applied to the target containing subimages before feature extraction to improve the performance of ATR. The same approach can also be employed in small target detection (STD) in SAR images. In such applications, detection can be done in two stages: the first prescreening stage filters out the suspicious subimages using fast detection algorithms which are set to have a high detection rate at the sacrifice of false alarms; the second false alarm mitigation (FAM) stage uses image enhancement and pattern classification of the features extracted from the enhanced subimages to mitigate the false alarms. This two stage approach has proven to be very effective for STD in SAR images.

However, the operation condition and task of STD are different from those of ATR. STD normally works on the SAR images of lower resolution and contrast, and its task is to discriminate targets from backgrounds, which requires less information of target shapes. As a result of these differences, the image features used for FAM in STD are generally different from those of ATR, and the requirements on image enhancement for STD may not be the same as those for ATR. Thus, the ATR results reported in the literature may not be directly applicable to STD.

The investigation presented in this paper compares different image enhancement methods and evaluates their im-

pact on FAM in STD, which provides a deeper insight into SAR image enhancement for STD in SAR images.

## 2. SAR IMAGE ENHANCEMENT ALGORITHMS

The SAR image enhancement algorithms considered in this paper are multi-look processing, Minimum Variance (MV) and Multiple SInal Classification (MUSIC) algorithms [4, 5]. These algorithms have proven to be effective for speckle reduction and resolution improvement [4] and are not computationally too heavy, hence can be tested on large data-sets relatively easily. Also, from low to high in the order of appearance, these algorithms provide different level of background suppression, therefore, the effect of background suppression on target and background discrimination can be compared using these algorithms.

### Multi-look processing

Fig 1 illustrates the steps of multi-look processing for generating a 4-look image. In the figure,  $x \in \mathcal{C}^{N \times N}$  is a given complex SAR image, and  $X \in \mathcal{C}^{N \times N}$  its phase history which can be obtained by a 2D FFT (FFT2) of  $x$  and the subsequent removal of any aperture weighting that may have been applied to form  $x$ . By hologram property [5], each piece of the phase history is sufficient to reconstruct an image of the entire scene. Thus  $m$  looks of the same scene can be created by evenly subdividing its phase history into  $m$  pieces and performing inverse FFT2 (IFFT2) on these pieces. Incoherent sum of these looks gives an intensity only real image of the scene with reduced speckle, which is called multi-look image. The more looks used, the more reduction of speckle. Compared with the image formed by IFFT2 of the entire phase history, the resolution of this multi-look image is  $\sqrt{m}$  times lower, and its size (number of pixels) is  $m$  times smaller. The interpolation performed with IFFT2 is to generate an image with same or larger size. In our investigation it is performed by zero padding  $X_i$  on all sides, so that the resulting array is a factor of  $k$  ( $k = 4$  in Fig 1) larger than the original  $X_i$ . The individual looks  $x_i$  are generated by IFFT2 of these zero padded arrays.

Usually, multi-look technique is used in SAR imaging only when the aperture over which the data is collected is significantly large [5] so that the image resolution is not compromised too much. As the size of sub-images to be

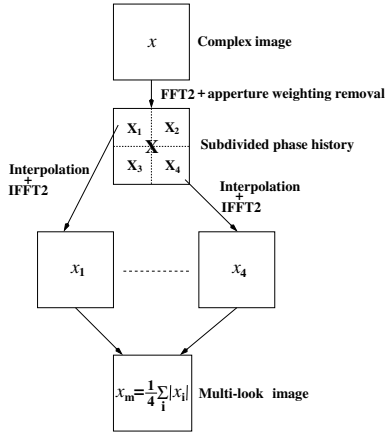


**Fig 1:** Multi-look processing

classified at FAM is relatively small and a relatively large number of looks is required for effective speckle reduction, the size of each subdivided phase history piece that is used to form an individual look is even smaller. Therefore, the resolution of the images enhanced with this technique will be much lower than the original ones. This may cause the small targets adjacent to each other within an sub-image being merged into a single bigger target. However, the task of FAM is to determine whether or not the central pixels of a given sub-image belong to target/s (this is always true since in practice the sub-images can always be cut out around the central pixels detected by prescreening), and identification of the number of targets is not required. As long as the intensity of the merged targets are strong enough in the multi-look image, the lower resolution might not be adverse to FAM. This has been confirmed by the experiment results presented in Section 4.

#### MV algorithm

Let  $X \in \mathcal{C}^{N \times N}$  be the phase history of a given complex image  $x \in \mathcal{C}^{N \times N}$ ,  $X_i \in \mathcal{C}^{n \times n}$  be a subblock of  $X$  with  $n \leq N$ ,  $Y \in \mathcal{C}^{n^2}$  be the data vector formed by column ordering of  $X_i$ ,  $R \in \mathcal{C}^{n^2 \times n^2}$  be the correlation matrix of  $Y$ ,  $M \times M$  be the required output image size, and  $W(k, l) \in \mathcal{C}^{n \times n}$  be the matrix defined as  $W(k, l) = [w_{ij}(k, l)]_{i,j=1,2,\dots,n} := [\exp(I\frac{2\pi}{M}(ik + jl))]_{i,j=1,2,\dots,n}$ , where  $I = \sqrt{-1}$ . The  $kl$ -th pixel of the MV image is given by

$$x_{kl} = \frac{1}{V^*(k, l)R^{-1}V(k, l)}, \quad k, l = 1, 2, \dots, M, \quad (1)$$

where  $V(k, l) \in \mathcal{C}^{n^2}$  is the vector formed by column ordering of  $W(k, l)$  and  $*$  denotes conjugate transpose. Normally,  $M \geq n$ . When  $M > n$ , the algorithm performs also interpolation, and the interpolation factor  $k = M/n$ . The images generated by MV algorithm (1) are intensity only real images.

The correlation matrix  $R$  is estimated from the given phase history data  $X$ . To get a full rank estimate of  $R$ , the subblocks contiguous to  $X_i$  are used. The number of subblocks is chosen such that it equals at least  $n^2$ , the rank

of  $R$ . As  $X$  is the only data available, the size of  $X_i$ ,  $n \times n$ , cannot be too large, otherwise, there will not be enough subblocks available. On the other hand, for better resolution,  $n$  should be as large as possible. To alleviate this difficulty, the forward and backward averaging [4] is employed to double the number of subblocks that can be used to estimate  $R$ . Specifically, let  $Y_i$  be the data vector of the  $i$ -th subblock  $X_i$ ,  $m \geq n^2/2$  be the total number of contiguous subblocks within  $X$ , and  $\hat{R}$  be the estimate of  $R$ . The forward and backward averaging is given by  $\hat{R} = \frac{1}{2m} \sum_{i=1}^m (Y_i Y_i^* + J Y_i^* Y_i^T J)$ , where  $J$  is the matrix obtained by rotating  $90^\circ$  an identity matrix with compatible dimension. The contiguous subblocks are formed using a sliding window of size  $n \times n$ , and the subblock size is  $40\% - 60\%$  of the full size of  $X$  [4]. The  $\hat{R}$  thus estimated replaces the  $R$  in MV algorithm (1).

The computation complexity of MV algorithm is on the order of  $n^6$  [4], that makes the algorithm too heavy to perform even for a small image of size  $64 \times 64$  and a  $40\% - 60\%$  subblock size. To alleviate this difficulty, the mosaicing strategy [4] shown in Fig 2 is used: The original image  $X$  is first subdivided evenly into  $p^2$  overlapping subimages, FFT2 and the subsequent removal of aperture weighting are performed on each subimage to recover its phase history; the phase history of each subimage is processed with MV algorithm (1) to generate the enhanced subimages; the enhanced subimages are mosaiced back after trimming off the overlap borders to composite a complete enhanced image. Using this strategy, the computation complexity for each subimage drops by a factor of  $p^6$ . For serial computation of the  $p^2$  subimages, which is used in our investigation, the overall improvement factor is  $p^4$  [4].

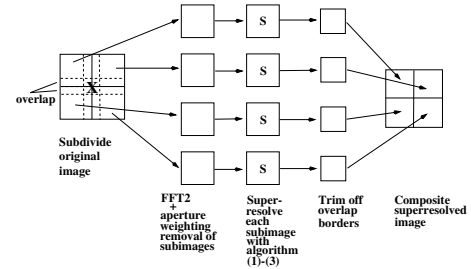


**Fig 2:** Mosaicing strategy

#### MUSIC algorithm

MUSIC algorithm uses the formula below to calculate the  $kl$ -th pixel of the enhanced image.

$$x_{kl} = \frac{1}{\frac{1}{C} \sum_{i=r+1}^{n^2} V^*(k, l) e_i e_i^* V(k, l)}. \quad (2)$$

In the above formula,  $r$  is the dimension of signal subspace [4, 6],  $V(k, l)$  is as defined in MV algorithm,  $e_i$  is the  $i$ -th singular vector of  $\hat{R}$  as described in MV algorithm, and  $C$  is given by [4]  $C = \frac{\sum_{i=r+1}^{n^2} \lambda_i}{n^2 - r - 1}$ . The implementation of MUSIC algorithm is similar to that of MV algorithm, which

involves all the steps shown in Fig 2, calculation of  $\hat{R}$ , plus singular value decomposition of  $\hat{R}$ .

### 3. TESTING THE ALGORITHMS

The three algorithms discussed in Section 2 have been tested on the complex SAR image data-sets. The testing results are presented below using six representative examples. These examples are selected from the 27, 226  $\times$  3 false alarm and 1, 434  $\times$  3 target image chips enhanced respectively by the three algorithms. All the original image chips are obtained from precreening large spotlight SAR images formed by the traditional IFFT2 of phase history data, with resolution  $\geq 1$  m. The size of the image chips is 64  $\times$  64, and the targets are vehicle type objects with size less than 8  $\times$  8 pixels centered at the position (32,32) of the image chips. As the aperture weighting used in forming these images are not known, it is assumed that no aperture weighting had been applied in image formation. Therefore, the FFT2 of these complex image chips are used as their phase histories. The examples of all three algorithms use the same target and false alarm image chips, so that direct comparison of these algorithms can be made. The following setups are used in the tested algorithms.

*Multi-look processing:* The recovered phase history is subdivided into 16 blocks with same size 4  $\times$  4. Each block is further interpolated to a factor of 16 and IFFT2-ed to form 16 looks of size 64  $\times$  64, which are incoherently summed to form the 16-look image.

*MV and MUSIC algorithms:* The central 50  $\times$  50 pixels of the original image chips are subdivided into  $p^2 = 25$  overlapping subimages; the size of each subimage is 12  $\times$  12, with 1 pixel overlap on all sides, and the FFT2 is performed on each subimage to recover its phase history; the size of subblocks used in calculating  $\hat{R}$  is 6  $\times$  6, and the size  $M \times M$  of each enhanced output subimage is 12  $\times$  12, ie the interpolation of a factor of 2 has been incorporated in MV and MUSIC algorithms; the 1 pixel border is trimmed off on all sides of the enhanced output subimages, and the remaining 10  $\times$  10 central pixels of these enhanced subimages are mosaiced together to composite a 50  $\times$  50 enhanced image. Under the above settings, the dimension of  $\hat{R}$  is 36  $\times$  36, and there are  $m = 49$  subblocks available for each (forward/backward) direction and a total of 98 subblocks for forward-backward averaging, which guarantees the non-singularity of  $\hat{R}$ . For MUSIC algorithms,  $r = 9$  is chosen as the dimension of signal subspace, which was estimated using empirical data and Akaike information criterion [4].

Fig 3 gives the original target and false alarm images and their enhanced counterparts. As can be seen, in all the enhanced images, the speckle has been significantly reduced. In the enhanced false alarm images, the central false alarm pixels become dimmer; in the enhanced target images, the target becomes more pronounced. In MV and MUSIC images, the target becomes much sharper. Fig 4 compares the 3D intensity mesh of the original and MUSIC enhanced target images. It can be seen that the background floor of MUSIC image is almost completely flat, showing a

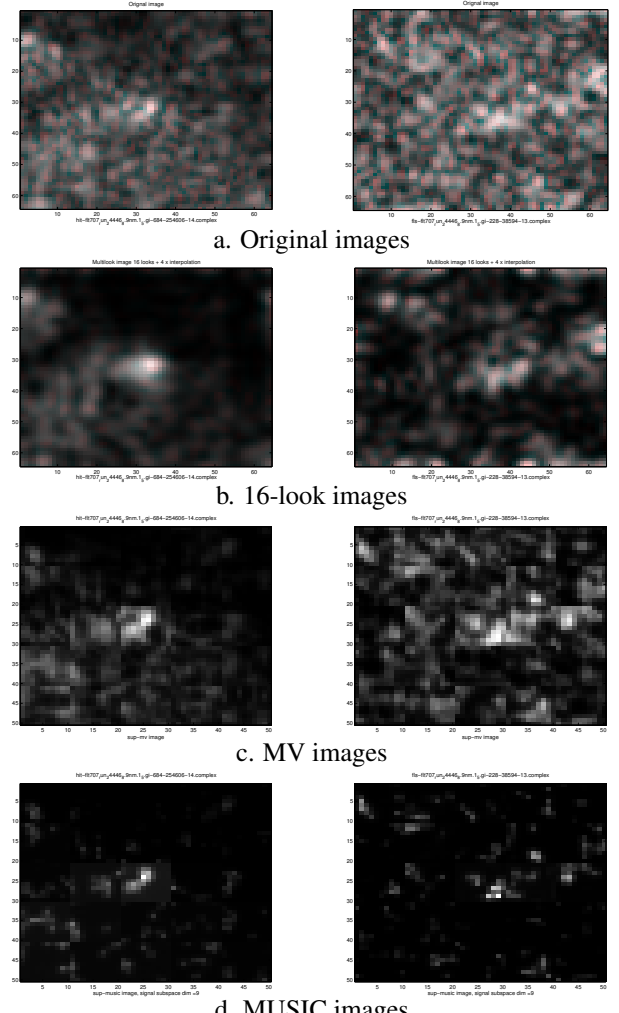


**Fig 3:** Original and enhanced images  
left: target, right: false alarm

very significant background noise reduction.

In the order of appearance, the three algorithms provide different level of background suppression. Multi-look provides the lowest level suppression and MUSIC the highest. The level of background suppression is an important affecting factor in visualization. If the background is suppressed too much, the terrain texture in the image background will be destroyed and the enhanced image will have lost its resemblance to the original image. In the extreme case, such as the MUSIC images given in Fig 3d, the background becomes almost invisible. Definitely, this is not desired if a better visualization is the main purpose of image enhancement. Therefore, the algorithms such as MUSIC which significantly suppress the backgrounds are not recommended in the literature for SAR image enhancement [4]. However, a better visualization does not necessarily imply a better discrimination of target and background. From the view point of detection, the images with only bright target spots and completely dark backgrounds might be the best.

### 4. FAM USING ENHANCED SAR IMAGES

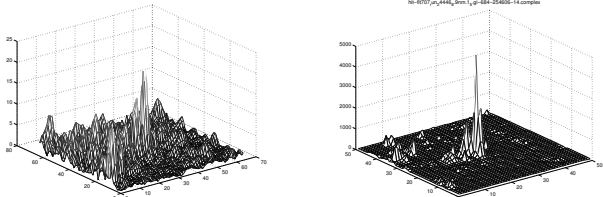


**Fig 4:** 3D intensity mesh of target images  
left: original, right: MUSIC

Two sets of SAR image data were used to investigate the impact of image enhancement on FAM. The images contained in the two data-sets are exactly same, except one set is the complex data of the images and the other is the intensity only real data. Each set contains 27, 226 false alarm and 1, 434 target chips with the same size  $64 \times 64$ . The three algorithms with the setups given in Section 3 were applied respectively to each image chip of the complex data-set to create three data-sets of enhanced image chips (referred to as enhanced data-sets). As the images generated by the three algorithms are all intensity only real images, the performance of FAM achieved on the enhanced data-sets is compared with that obtained from the non-enhanced intensity only real data-set (referred to as non-enhanced data-set).

The same image features were extracted from the image chips of the three enhanced data-sets and the non-enhanced data-set. The features from the same data-set were classified using a Fisher linear discriminant to discriminate the targets from false alarms. The classifier was trained with 40% of the feature data. The features used are the five best features selected on the non-enhanced data-set, these are the image mean, the  $(1, 2)$ -th coefficient of the FFT2 of the images, and three co-occurrence matrix features. Because the co-occurrence matrix features are sensitive to image mean, a search of the best value for shifting image mean was performed on each data-set. The reason for doing so is to compare the best performance achievable on each data-set using the same features.

Given in Table 1 are the probabilities of false alarm  $P_{fa}$  at the probabilities of detection  $P_d = 90\%$  achieved on different data-sets. Compared with the non-enhanced data-set, all the enhanced data-sets provide significant performance improvement. Among the three enhanced data-sets, MUSIC enhanced data-set gives the highest performance: at  $P_d = 90\%$ ,  $P_{fa} = 1.2277\%$ , which is 3.65 times lower than that of the non-enhanced data-set.

| MUSIC   | MV      | Multi-look | Non-enhanced |
|---------|---------|------------|--------------|
| 1.2277% | 1.5734% | 2.1242%    | 4.4828%      |

**Table 1:**  $P_{fa}$  at  $P_d = 90\%$  achieved on different data-sets

## 5. CONCLUSIONS AND DISCUSSIONS

Three algorithms for SAR image enhancement have been used to investigate the impact of image enhancement on the false alarm mitigation of small target detection in SAR images. The testing results show that image enhancement im-

proves greatly the performance of false alarm mitigation and that the best performance improvement achieved on tested data-set is a 3.65 times reduction of  $P_{fa}$  at  $P_d = 90\%$ .

The testing results also show that compared with ATR, STD requires different properties from image enhancement. As the purpose of image enhancement for STD is target and background discrimination but not visualization, the algorithms such as MUSIC, which does not provide good visualization and is not recommended in the literature for SAR image enhancement [4], can actually provide better performance of small target detection in SAR images. The level of performance improvement is correlated with the resolution and background suppression of the enhanced images. The higher the resolution and the level of background suppression, the higher the level of performance improvement.

## References

- [1] Bi, Z., J. Li and Z. Liu, Super resolution SAR image formation via parametric spectral estimation methods, *Proc SPIE*, Vol. 3370, pp. 238-249, 1998.
- [2] Bernitz, G. R., High-definition vector imaging, *Lincoln Laboratory Journal*, Vol. 10, No 2, pp. 147-170, 1997.
- [3] Brito, A E, Chan, S H and Cabrera, S D, SAR image formation using 2d re-weighted minimum norm extrapolation, *Proc SPIE*, Vol. 3721, pp. 78-91, 1999.
- [4] DeGraaf, S., SAR imaging via modern 2d spectral estimation methods, *IEEE Trans IP*, Vol 7, No 5, pp 729-761, 1998.
- [5] Jakowatz, C. V., Jr. D.E. Wahl, P. H. Eichel, D. C. Ghiglia and P. A. Thompson, *Spotlight-mode Synthetic Aperture Radar: A Signal Processing Approach*, Kluwer Academic Publishers, 1996.
- [6] Marple, S.L. *Digital Spectral Analysis*, Prentice Hall, 1987.
- [7] Novak, L. M., G. J. Owirka, W. S. Brower and A. L. Weaver, The automatic target recognition system in SAIP, *Lincoln Laboratory Journal*, Vol. 10, No 2, pp. 187-202, 1997.
- [8] Owirka, G.J., A. L. Weaver and L. M. Novak, Performance of a multi-resolution classifier using enhanced resolution SAR data, *Proc SPIE*, Vol. 3066, pp. 90-100, 1999.
- [9] Owirka, G.J., Verbout, S.M. and Novak, L.M., Template-based SAR ATR performance using different image enhancement techniques, *Proc SPIE*, Vol. 3721, pp. 302-319, Apr, 1999.